

Supporting Information

Interfacial Assembly of Metal–Phenolic Networks for Hair Dyeing

*Huimin Geng,[†] Liping Zhuang,[†] Mengqi Li,[†] Hanru Liu,[†] Frank Caruso,^{†,§} Jingcheng Hao,[†]
Jiwei Cui^{†,‡,*}*

[†]Key Laboratory of Colloid and Interface Chemistry of the Ministry of Education, School of Chemistry and Chemical Engineering, Shandong University, Jinan, Shandong 250100, China

[‡]State Key Laboratory of Microbial Technology, Shandong University, Qingdao, Shandong 266237, China

[§]ARC Centre of Excellence in Convergent Bio-Nano Science and Technology, and the Department of Chemical Engineering, The University of Melbourne, Parkville, Victoria 3010, Australia

* Corresponding authors: jwcui@sdu.edu.cn

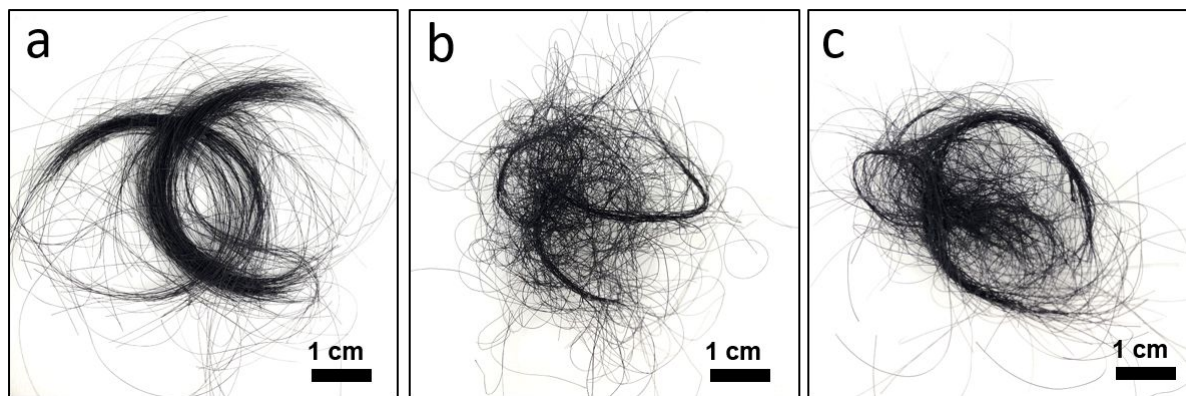


Figure S1. Photographs of tannic acid (TA)-Fe(II)-coated commercial gray hair samples subjected to a number of washes: (a) 0, (b) 25, and (c) 50.

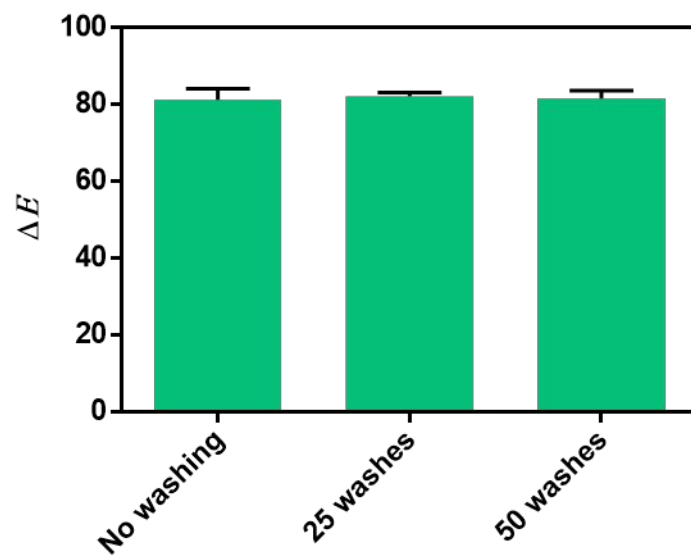


Figure S2. The color difference (ΔE) values of TA-Fe(II)-coated commercial gray hair samples subjected to a number of washes.

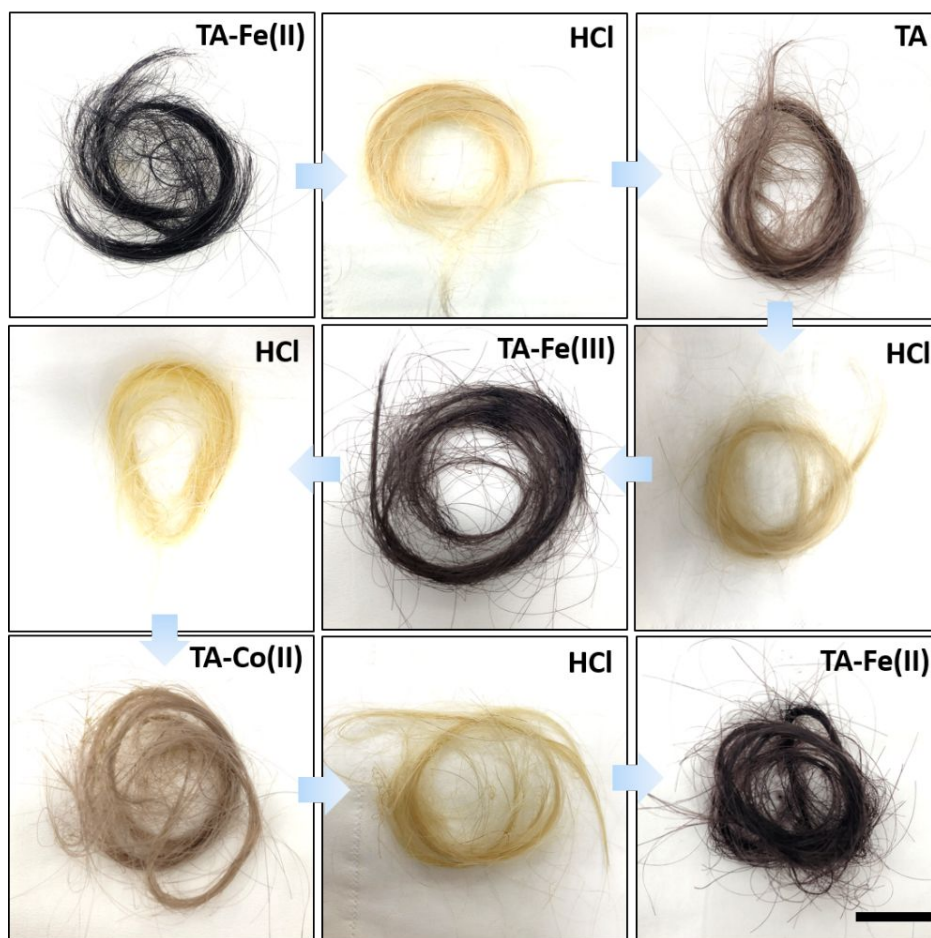


Figure S3. Photographs of commercial gray hair samples subjected to sequential dyeing/discoloration processes (scale bar = 1 cm). Discoloration was achieved with HCl.

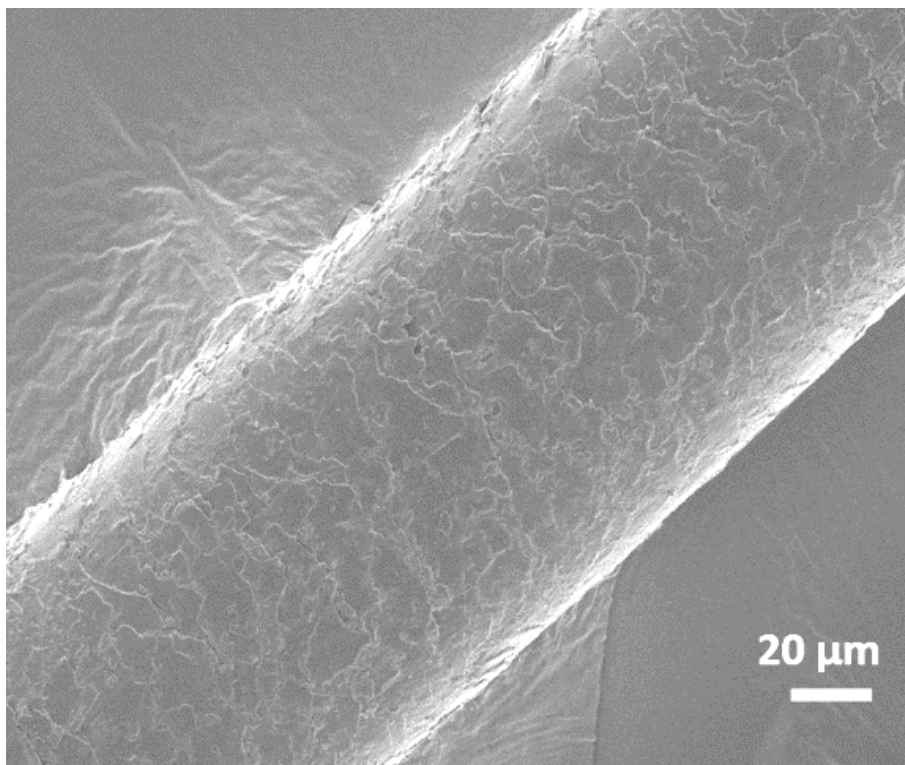


Figure S4. Scanning electron microscopy (SEM) image of a TA-coated commercial gray hair fiber.

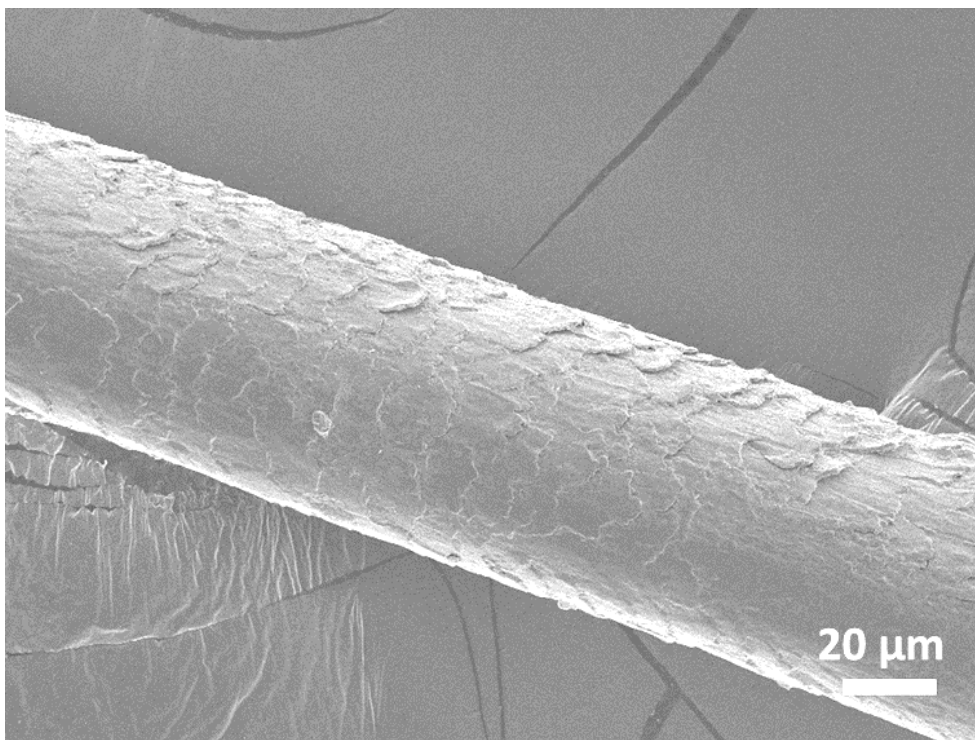


Figure S5. SEM image of a TA-Fe(II)-coated commercial gray hair fiber after 50 shampoo washes.

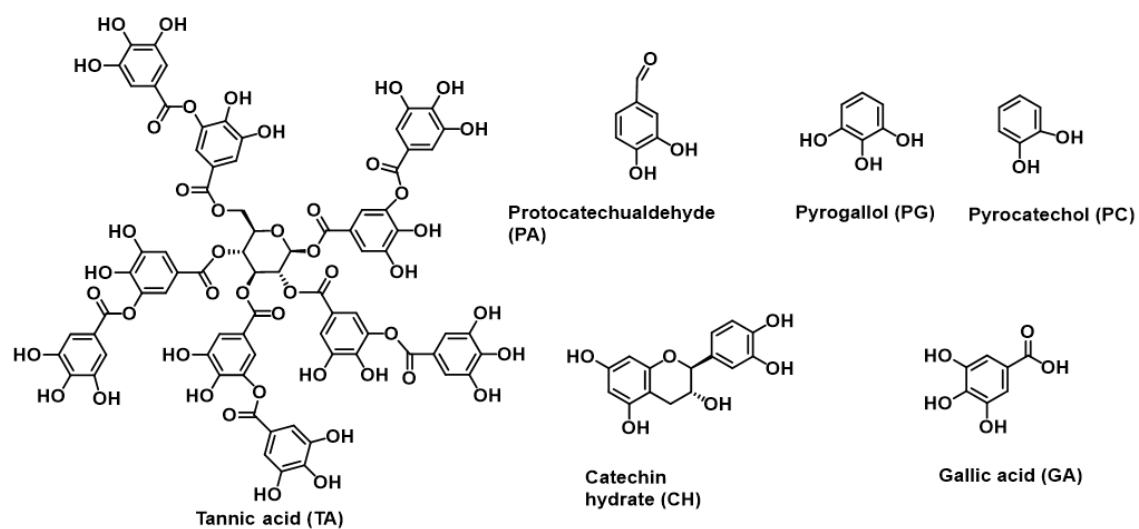


Figure S6. Structures of the different polyphenols examined in this study.



Figure S7. Photographs of human natural (non-commercial) gray hair subjected to repeated coating (dyeing) with GA-Fe(II).

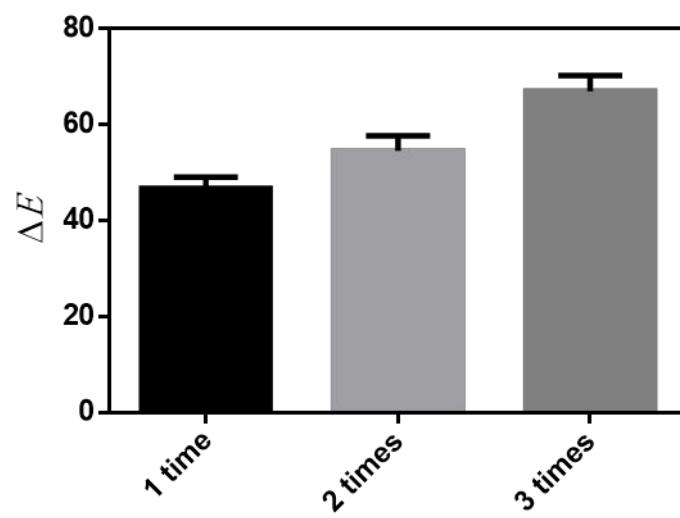


Figure S8. ΔE of human natural gray hair subjected to repeated coating with GA-Fe(II).



Figure S9. Photograph of human natural gray hair samples coated with GA-Fe(II) at different precursor (ligand-to-metal) molar ratios. The concentration of GA was fixed at 5 mg mL⁻¹.

Uncoated pH 1.5 pH 3.5 pH 4.5 pH 5.5 pH 6.5 pH 7.4



Figure S10. Photograph of human natural gray hair samples coated with GA-Fe(II) and at different pH (GA-to-Fe molar ratio was 1:5).

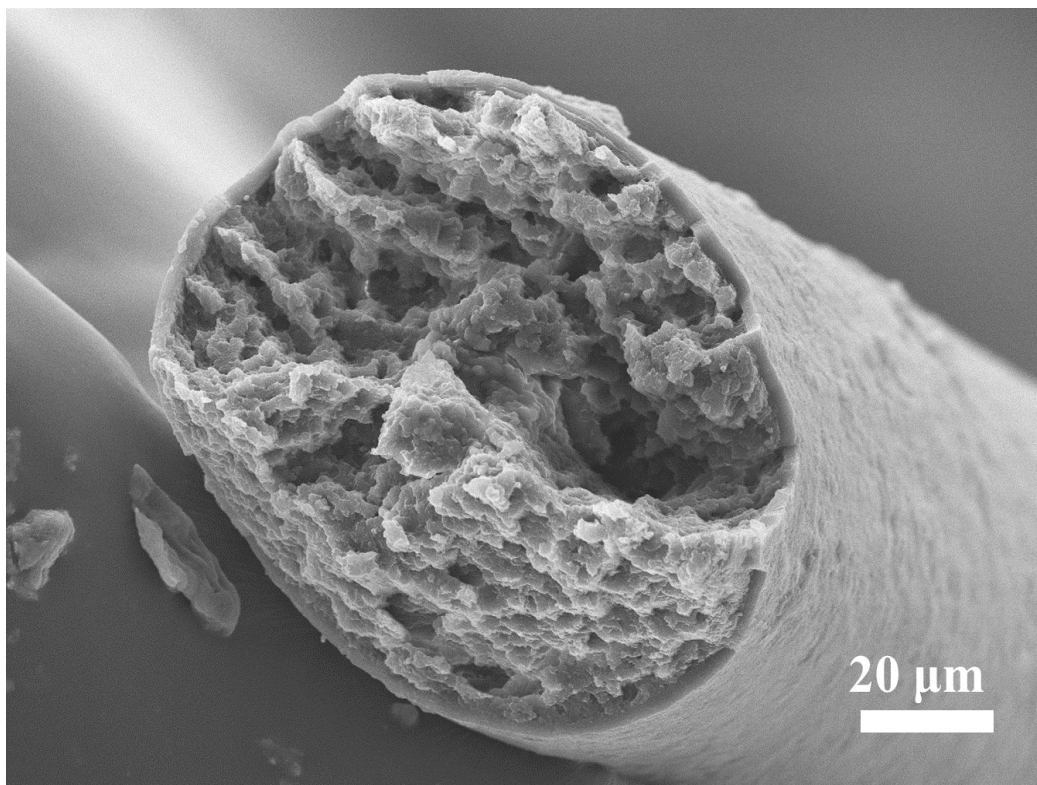


Figure S11. SEM image of the cross-section of a human natural gray hair fiber coated with GA-Fe(II).

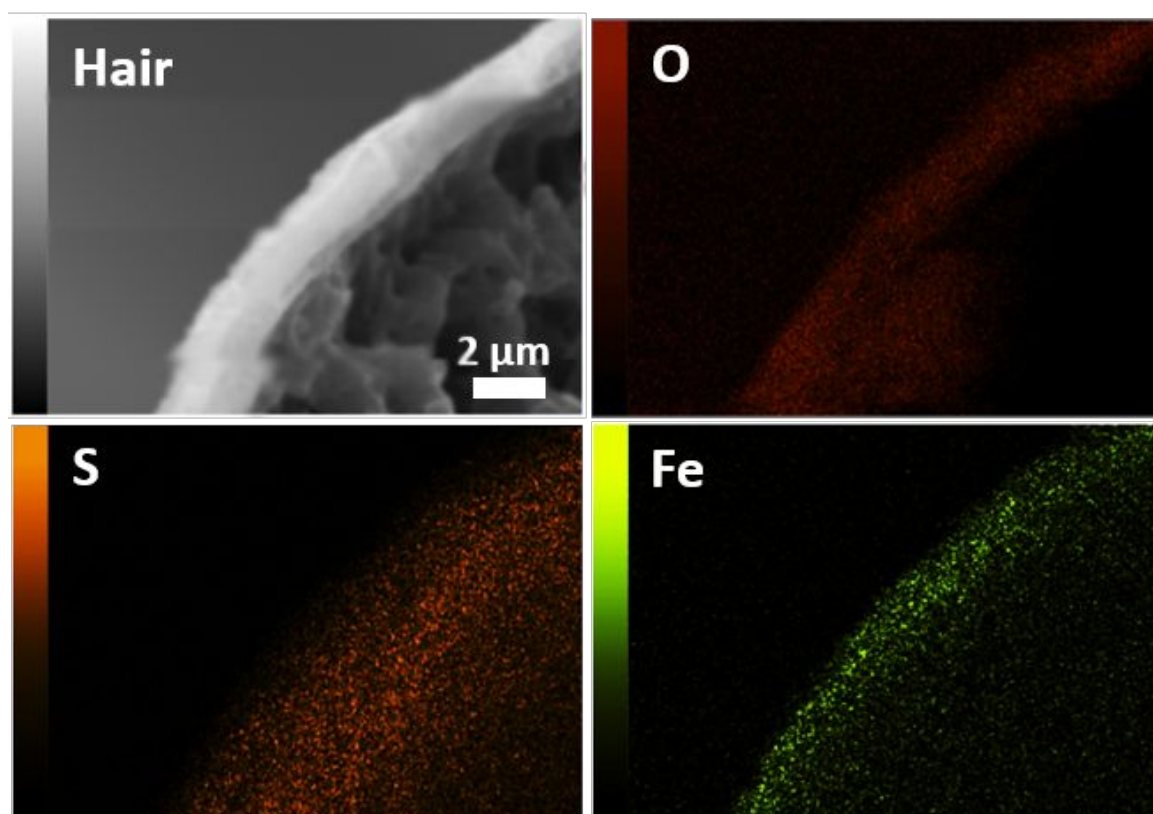


Figure S12. Energy-dispersive X-ray spectroscopy (EDS) mapping images of the cross-section of a human natural hair fiber coated with GA-Fe(II), showing the presence of elements O, S, and Fe.



Figure S13. Photograph of GA-Fe(II)-coated human natural gray hair samples subjected to a number of shampoo washes at room temperature.

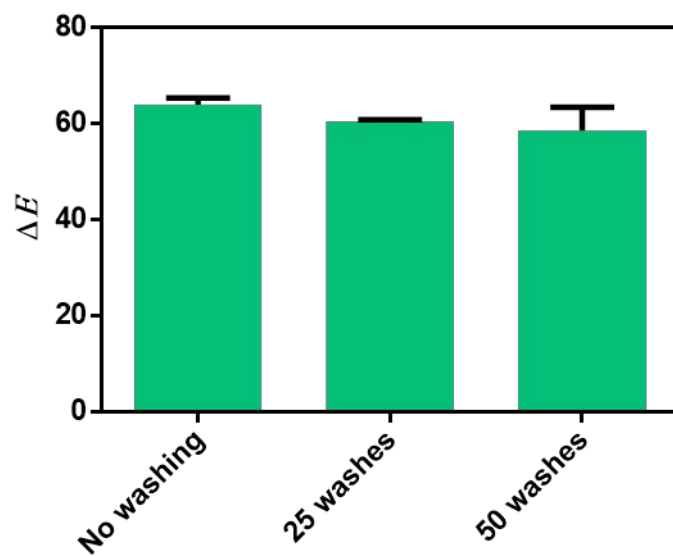


Figure S14. ΔE of human natural gray hair samples coated with GA-Fe(II) and subjected to a number of shampoo washes at 25 °C.

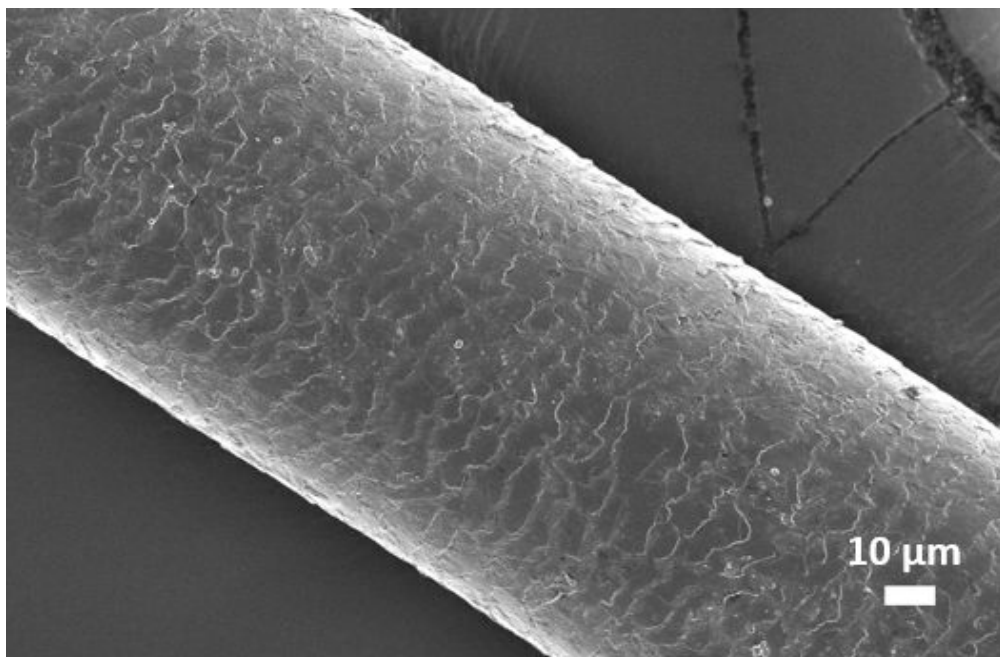


Figure S15. SEM image of a GA-Fe(II)-coated human natural gray hair fiber after 50 washes with shampoo at 25 °C.



Figure S16. Photographs of GA-Fe(II)-coated human natural gray hair subjected to 50 shampoo washes at 45 °C.



Figure S17. Photographs of GA-Fe(II)-coated human natural gray hair before and after treatment with boiling water for 1 h.



Figure S18. Photographs of GA-Fe(II)-coated human natural gray hair before and after sunlight exposure for 7 days.



Figure S19. Photograph of GA-Fe(II)-coated human natural gray hair samples after immersion in different pH solutions for 12 h.

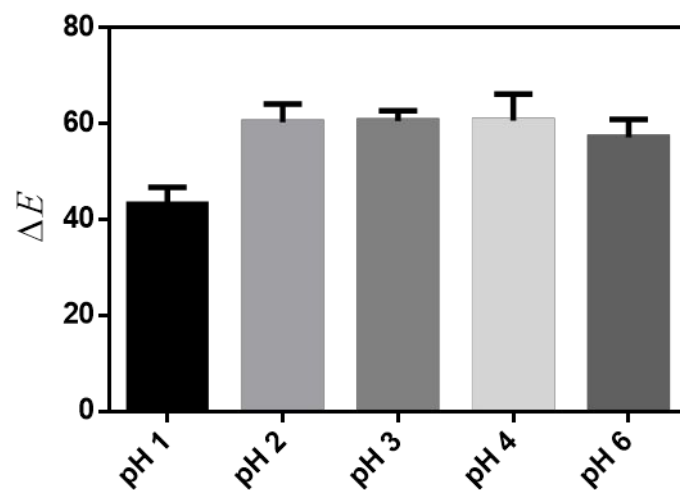


Figure S20. ΔE of GA-Fe(II)-coated human natural gray hair samples after immersion in different pH solutions for 12 h.

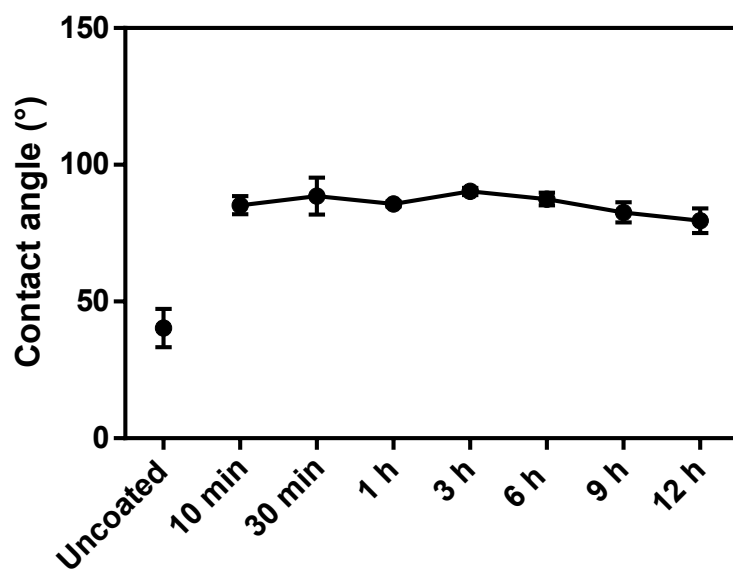


Figure S21. Water contact angles of quartz substrates before (uncoated) and after coating with GA-Fe(II) subjected to coating time.

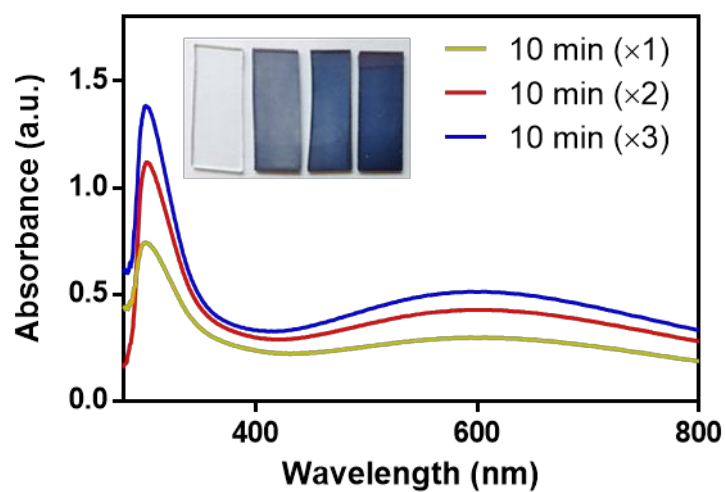


Figure S22. UV-vis absorbance spectra of quartz substrates with GA-Fe(II) coatings subjected to a number of coatings.

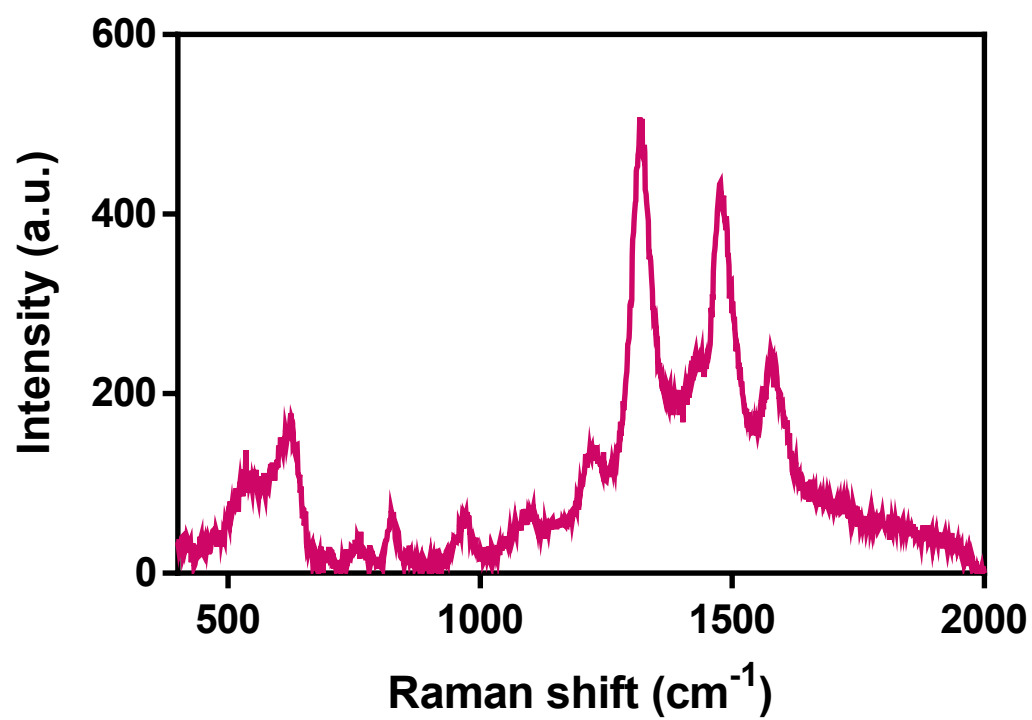


Figure S23. Resonance Raman spectrum of the surface of the GA-Fe(II) interfacial film.

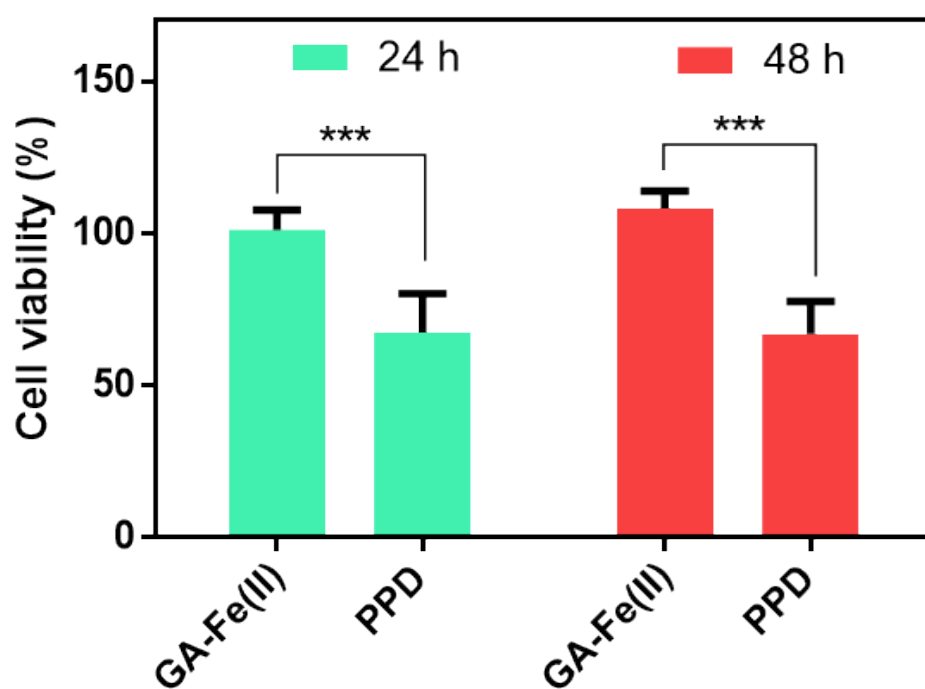


Figure S24. Cell cytotoxicity evaluations of GA-Fe(II)-treated hair extracts and *p*-phenylenediamine (PPD)-treated hair extracts against mouse embryonic fibroblast cells (NIH-3T3) after incubation for 24 and 48 h (** $P < 0.0001$).

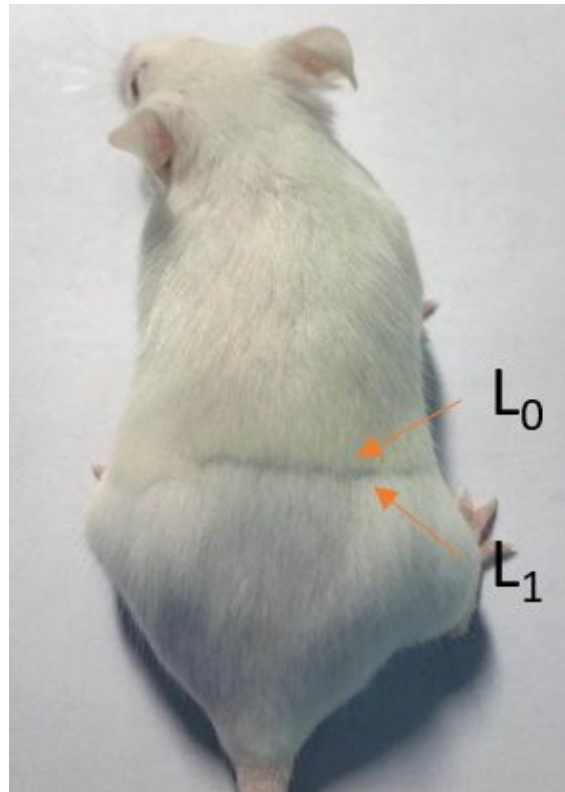


Figure S25. Photograph of a mouse model depicting L_1 and L_0 .

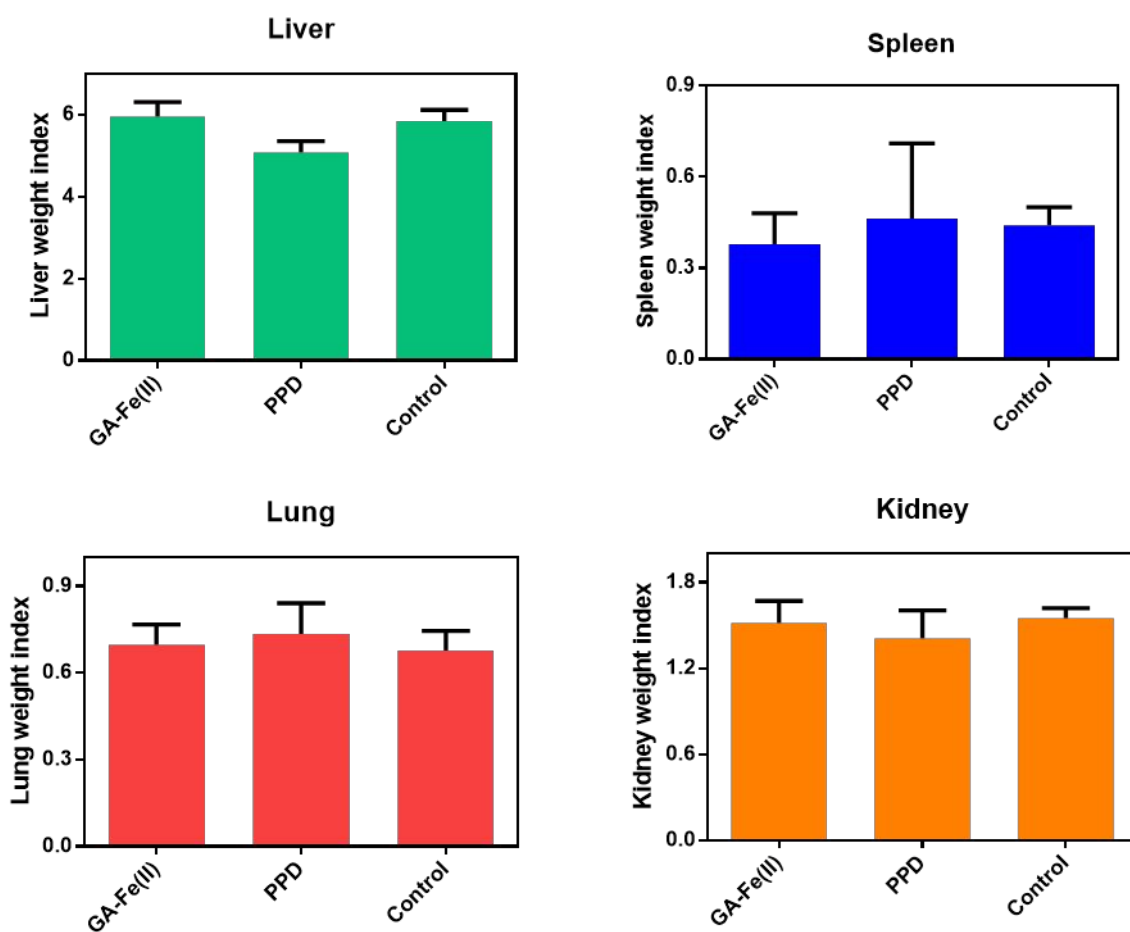


Figure S26. Effect of GA-Fe(II) and PPD treatment on the viscera index of spleen, lung, liver, and kidney on mice.